A PV View of the Zonal Mean Distribution of Temperature and Wind in the Extratropical Troposphere

DE-ZHENG SUN

Program in Atmospheric and Oceanic Sciences, Princeton University, Princeton, New Jersey

RICHARD S. LINDZEN

Center for Meteorology and Physical Oceanography, Massachusetts Institute of Technology, Cambridge, Massachusetts

(Manuscript received 1 April 1993, in final form 16 August 1993)

ABSTRACT

The dependence of the temperature and wind distribution of the zonal mean flow in the extratropical troposphere on the gradient of potential vorticity along isentropes is examined. The extratropics here refer to the region outside the Hadley circulation. Of particular interest is whether the distribution of temperature and wind corresponding to a constant PV along isentropes resembles the observed, and the implications of PV homogenization along isentropes for the role of the tropics.

With the assumption that PV is homogenized along isentropes, it is found that the temperature distribution in the extratropical troposphere may be determined by a linear, first-order partial differential equation. When the observed surface temperature distribution and tropical lapse rate are used as the boundary conditions, the solution of the equation is close to the observed temperature distribution except in the upper troposphere adjacent to the Hadley circulation, where the troposphere with no PV gradient is considerably colder. Consequently, the jet is also stronger. It is also found that the meridional distribution of the balanced zonal wind is very sensitive to the meridional distribution of the tropopause temperature. The result may suggest that the requirement of the global momentum balance has no practical role in determining the extratropical temperature distribution.

The authors further investigated the sensitivity of the extratropical troposphere with constant PV along isentropes to changes in conditions at the tropical boundary (the edge of the Hadley circulation). It is found that the temperature and wind distributions in the extratropical troposphere are sensitive to the vertical distribution of PV at the tropical boundary. With a surface distribution of temperature that decreases linearly with latitude, the jet maximum occurs at the tropical boundary and moves with it. The overall pattern of wind distribution is not sensitive to the change of the position of the tropical boundary.

Finally, the temperature and wind distributions of an extratropical troposphere with a finite PV gradient are calculated. It is found that the larger the isentropic PV gradient, the warmer the troposphere and the weaker the jet.

1. Introduction

The importance of the potential vorticity (PV) distribution along isentropes in the extratropical large-scale dynamics has long been recognized and emphasized (Charney and Stern 1962; Hoskins et al. 1985). It has also been proposed that the PV may be a powerful diagnostic tool for studying the general circulation (Hoskins 1991). However, it appears that no adequate efforts have been made to examine the temperature and wind distribution of the zonal mean flow as a function of PV distribution along isentropes.

The need to examine the dependence of the zonal mean flow on the PV distribution along isentropes was further highlighted by Lindzen (1993). Lindzen noted that, given the meridional confinement of the baroclinic instabilities by the subtropical jet (leading to a finite minimum horizontal wavenumber), it was possible to neutralize the atmosphere by eliminating pseudo PV gradients along isobars (or equivalently PV gradients along isentropes) above the surface to a sufficiently great height, corresponding to the tropopause. The relevance of such a neutral state to the real atmosphere is dependent on whether the temperature and wind distribution corresponding to a constant PV along isentropes resembles the observed. It should be noted that while baroclinic instability may plausibly act to bring the basic state *toward* neutrality, one cannot reasonably suppose that neutrality will be fully achieved. Rather, a balance is achieved between the generation of eddies and their dissipation by linear and nonlinear processes. The present study offers some evidence that the neutral state may nonetheless offer a reasonable approximation for some purposes.

Corresponding author address: Dr. Richard S. Lindzen, Center for Meteorology and Physical Oceanography, MIT, Bldg. 54, Rm. 1720, Cambridge, MA 02139.

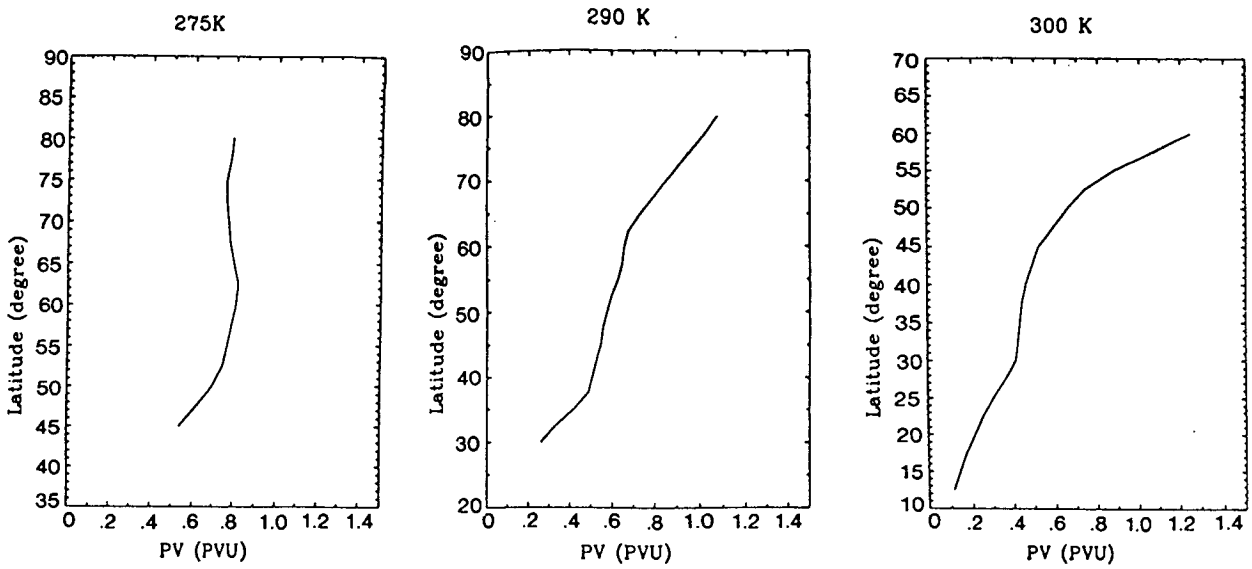

FIG. 1. Potential vorticity distribution (in PVU) along three representative isentropes (top: 290 K; bottom right: 300 K; bottom left: 275 K. 1 PVU = 10^{-6} m^2 s^{-1} K). Data source: 1963–73 climatology for the winter season of the Northern Hemisphere from Dr. A. Oort at GFDL. [The data tabulated in Oort (1983) produce spurious superadiabatic lapse rate below 950 mb. This problem was corrected in the new dataset used here.]

In this paper, we describe how to calculate the distribution of temperature and wind as a function of the PV distribution along isentropes. Motivated by Lindzen's note, we are particularly interested in whether there is any significant difference between the observed temperature and wind distribution and the one corresponding to a homogenized PV distribution along isentropes. We also examine the implications of PV homogenization along isentropes in the extratropical troposphere for the role of the tropics.

This paper is organized as follows. In section 2, we present the distributions of PV of the observed zonal mean flow, whose characteristic structures indeed indicate mixing in the interior of the extratropical troposphere. In section 3, we describe the calculation of the temperature and wind distribution of an extratropical troposphere with zero isentropic PV gradient and compare the result with the observed. In section 4, we investigate the sensitivity of the temperature and wind distribution in the extratropical troposphere to the tropical lapse rate and the position of the edge of the Hadley circulation. In section 5, we quantify the sensitivity of the temperature and wind distribution to the changes in the gradient of PV. Section 6 provides our summary.

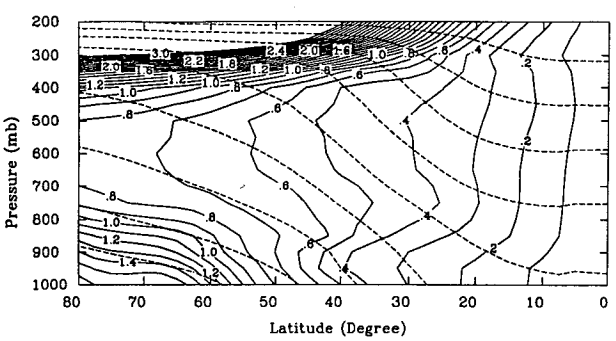

FIG. 2. Potential vorticity and potential temperature distributions in the troposphere for the winter season of the Northern Hemisphere. For clarity, isentropes are not labeled. The contours start from 260 K and end at 340 K with an even interval 10 K. Contours of PV end at 3.0 PVU. (Data source: same as in Fig. 1.)

2. The characteristic PV distribution of the observed flow

The expression for the isentropic PV is

$$P_v = -g(f + \zeta_\theta)\frac{\partial \theta}{\partial p} \tag{1}$$

in which g is the gravitational constant, f is the planetary vorticity, θ represents the potential temperature, p is the pressure, and ζ_θ is the relative vorticity evaluated along isentropes (Hoskins et al. 1985).

Figure 1 shows the PV distributions along three representative isentropes of the observed zonal mean flow of the winter season (290 K, 300 K, and 275 K, respectively). The 290-K isentrope originates from the subtropical surface and intersects the tropopause shortly before reaching the pole. The 300-K isentrope originates in the tropics and intersects the tropopause at about 60°N. The 275-K isentrope originates from the extratropical surface and passes over the pole without intersecting the tropopause. For reference purposes,

Fig. 2 presents the PV and potential temperature distributions of the winter season over the entire Northern Hemisphere.

It is apparent from Fig. 1 that the distribution of PV along isentropes is characterized by different regimes. The gradient of PV along the section of the isentropes that falls in the interior of the extratropical troposphere is distinguishably smaller than along the section that falls into either the Hadley regime, the immediate region of the ground, or the transitional region to the tropopause. Note that on the 300-K isentrope, the gradient of PV between 10°N and 30°N is clearly much larger than that between 30°N and 45°N, the section which lies in the interior of the extratropical troposphere. Also note that the 275-K isentrope has only a surface boundary layer since it reaches the pole without intersecting the tropopause. This characteristic distribution of PV indicates vigorous mixing in the interior of the extratropical troposphere.

For the zonal mean flow, the relative vorticity ζ_θ is an order of magnitude or more smaller than the planetary vorticity f. The chief contributor to the PV distribution is $-gf(\partial\theta/\partial p)$. This provides a convenient link between PV, which is conserved for adiabatic and inviscid flows, and lapse rate, which is not.

As is evident in Fig. 1, the isentropic gradient of PV in the troposphere appears to be distinguishable from zero. However, one should note that the change of PV from its surface values or tropical values to its stratospheric values is large, and consequently the PV gradient in the interior of the troposphere may be considerably exaggerated here due to the low resolution of the observational data. Data used here is the analyzed radiosonde data, which is only available at the standard pressure levels (Oort 1983). An effective way to check the significance of the PV gradient is to obtain the distribution of temperature and wind corresponding to a constant PV along isentropes, and then compare this distribution of temperature and wind with the observed. The major concern here is whether the assumption of PV homogenization along isentropes can provide a practical way to determine the distribution of temperature and wind. This is the subject of the following section.

3. An extratropical troposphere with a zero PV gradient

a. An approximate calculation

As shown by observations, for the time and zonal mean flow of the extratropical troposphere, the relative vorticity ζ_θ is one order of magnitude or more smaller than the planetary vorticity. Therefore, to first-order approximation, the PV is simply $-gf(\partial\theta/\partial p)$. This corresponds to the planetary-scale approximation (Pedlosky 1987). The same approximation has been made by oceanographers in their studies of the large-scale structure of the thermocline circulation (Luyten et al. 1983; Marshall and Nurser 1991). This greatly simplifies the calculation as we will see later. However, whether $\zeta_\theta \ll f$ is dependent on how the PV is distributed and what the boundary conditions for the temperature and wind are. When we take an idealized PV distribution that differs from that observed, this assumption may not be good. This can be easily checked once the temperature and wind distributions are obtained under this assumption.

Note that for any quantity $F = F(y, p)$, we have

$$\left(\frac{\partial F}{\partial y}\right)_\theta = \frac{\partial F}{\partial y} - \frac{\partial \theta}{\partial y}\left(\frac{\partial \theta}{\partial p}\right)^{-1}\frac{\partial F}{\partial p}, \tag{2}$$

where $y = a\phi$, a is the radius of the earth, ϕ represents the latitude, and p represent the pressure. Here θ is the potential temperature, which is a function of the latitude and pressure; $(\partial F/\partial y)_\theta$ is the derivative of F evaluated along isentropes.

Defining $P_a \equiv -gf(\partial\theta/\partial p)$, the gradient of P_a along isentropic surfaces can be written

$$-g^{-1}\left(\frac{\partial P_a}{\partial y}\right)_\theta = \frac{df}{dy}\frac{\partial\theta}{\partial p} + f\frac{\partial^2\theta}{\partial y\partial p} - f\frac{\partial\theta}{\partial y}\left(\frac{\partial\theta}{\partial p}\right)^{-1}\frac{\partial}{\partial p}\frac{\partial\theta}{\partial p}. \tag{3}$$

If P_a is constant along isentropic surfaces, we may rearrange (3) as

$$\frac{\partial}{\partial p}\frac{(\partial\theta/\partial y)}{(\partial\theta/\partial p)} = -\frac{1}{f}\frac{df}{dy}. \tag{4}$$

Integrating from the surface level p_s to the level p, we obtain the following equation for θ:

$$f\frac{\partial\theta}{\partial y} - \left[\frac{-gf^2}{P_{as}}\frac{\partial\theta_s}{\partial y} - \frac{df}{dy}(p - p_s)\right]\frac{\partial\theta}{\partial p} = 0, \tag{5}$$

where $P_{as} \equiv -gf(\partial\theta/\partial p)_s$; P_{as} and θ_s are the PV and potential temperature at the level of $p = p_s$. Note that relative vorticity is ignored.

Equation (5) is a first-order, linear partial differential equation. For a given θ_s, P_{as}, and a potential temperature distribution at the tropical boundary (the edge of the Hadley cell), Eq. (5) gives the temperature distribution of the entire extratropical troposphere. Solving Eq. (5) does not require knowledge of the tropopause height.

Once the temperature distribution is obtained, the zonal mean wind may then be estimated by the thermal wind relationship,

$$f\frac{\partial U}{\partial p} = \hat{R}\frac{\partial\theta}{\partial y}, \tag{6}$$

where $\hat{R} = [d\Pi(p)/dp]$; $\Pi(p)$ is the Exner function. For convenience, we take $U|_{p=p_s} = 0$.

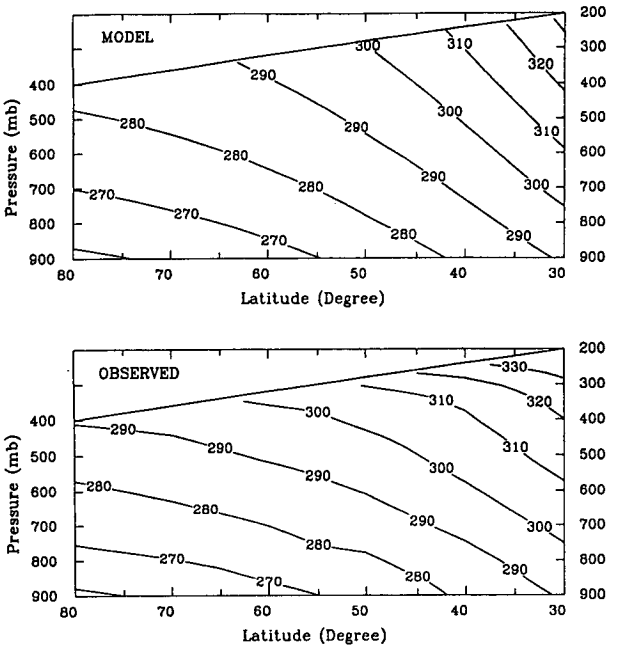

FIG. 3. Top: The potential temperature distribution obtained through Eq. (5). Temperature at 900 mb is maintained at the observed value for the winter season; P_{as} is taken from the observed value at 800 mb. Bottom: Observed zonal mean potential temperature distribution for the winter season (Oort 1983).

We solve Eq. (5) numerically by treating it as a typical transport equation with a varying coefficient (or velocity). The isentropes are the characteristic lines of Eq. (5). The details of the numerical procedure are presented in appendix A. A solution to Eq. (5) is shown in Fig. 3. The corresponding thermal wind distribution obtained through Eq. (6) is presented in Fig. 4. Presented also in Figs. 3 and 4 are the observed temperature and wind distributions for the winter season. In the calculation, we take p_s = 900 mb and maintain the potential temperature at 900 mb (θ_s) at the observed value. The PV distribution across the isentropes originating from the extratropical surface P_{as} is taken to be the same as the observed values at 800 mb (recall that above 850 mb and below the transitional region to the stratosphere, the observed PV distribution is only weakly dependent on height). The position for the tropical boundary is approximately where the winter Hadley cell ends (30°N). The temperature distribution at the tropical boundary is assumed to be linear with pressure. This is a good approximation for the interior troposphere. The value for $\partial\theta/\partial p$ is taken as the mean observed value between 900 and 300 mb at 30°N. This gives a vertically well-mixed PV when wind shear can be ignored. The solution is assumed to extend to a specified height that represents the tropopause level. This height is assumed to vary linearly from 200 mb at 30°N to 400 mb at 80°N.

The exact PV distribution corresponding to the temperature and wind distributions in Fig. 3 is presented in Fig. 5. Shown also in Fig. 5 is the PV distribution when the contribution from the relative vorticity is ignored. The difference between the two is small. The temperature and wind distributions presented at the top of Figs. 3 and 4 are the exact solutions we would get if we inverted the PV distribution given in the lower portion of Fig. 5 with the requirement of thermal wind balance. One may still wonder if the small difference can lead to a considerable difference in the balanced mass and momentum distribution. When the mass and momentum are balanced and PV is positive, both the wind and the temperature are related to the PV through an elliptic operator. Based on the smoothing property of the elliptic operator, we do not expect that the small-scale structure appearing in Fig. 5 will lead to any considerable difference in the temperature and wind distribution. We will address this issue in a more rigorous manner in the following section.

By comparing the solution with observations, this idealized solution appears to define much of the observed distribution with some significant discrepancy near the tropopause level, particularly in the region near the tropical boundary. The latitude that the isentropes originating from the tropics reach before they intersect the tropopause is somewhat smaller than is observed. An examination of Eq. (4) reveals that the slope of the isentropes increases with height due to the effect of β, the planetary vorticity gradient. So far as the latitude

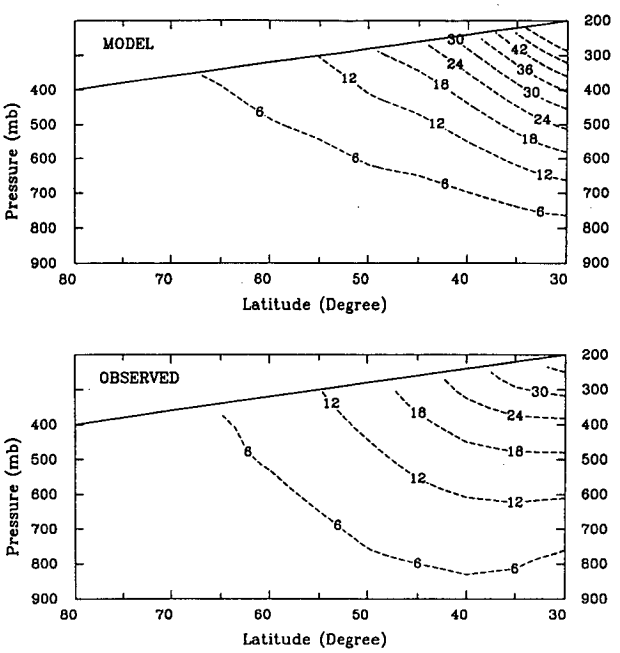

FIG. 4. Top: The zonal wind distribution obtained through Eq. (6). Bottom: Observed wind distribution for the winter season (Oort 1983).

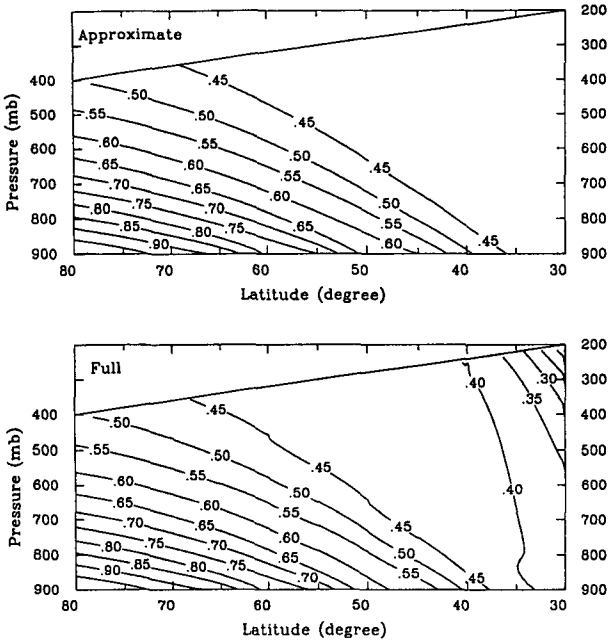

FIG. 5. Top: PV distribution when ζ_θ is ignored. Note that PV on isentropes that originate in the tropics has a uniform value of 0.43 PVU. Bottom: The PV (in PVU) distribution corresponding to the potential temperature and wind distributions in Figs. 3 and 4 (top).

that the isentropes originating from the tropics can reach before they reach the tropopause is concerned, it seems that efficient PV mixing along isentropes does not significantly increase the impact of the tropics on the extratropics. As a matter of fact, due to the existence of the planetary vorticity gradient, the extratropics will not have the same lapse rate as the tropics even when the PV in the extratropical troposphere is homogenized both vertically and horizontally. In that case, the extratropical lapse rate is connected with the tropical lapse rate simply by

$$f\frac{\partial\theta}{\partial p} = f_0\left(\frac{\partial\theta}{\partial p}\right)_0. \tag{7}$$

The subscript 0 denotes the position of the tropical boundary; ζ_θ is ignored in the above equation. For a surface temperature distribution similar to the present, calculations show that ignoring ζ_θ is a good approximation.

The extratropical troposphere with well-mixed PV along isentropes is colder than observed. Accompanying a colder upper troposphere and the larger slope of the isentropes originating from the tropics, the jet is also much stronger than that observed.

To the extent that the relative vorticity in the PV expression can be ignored, it seems that the temperature distribution in the extratropical troposphere can be determined without the need to know the tropopause height and the stratospheric temperature. However, the role of the stratosphere is implicit in the above formulation. The equilibrium value of PV on isentropes is expected to be dependent on the tropopause height and the radiative budget. We will investigate the sensitivity of the temperature and wind distribution to changes in the cross-isentrope PV distribution later. Next, we quantify the seemingly small effect of wind on the PV distribution. A more subtle role of the stratosphere in affecting tropospheric wind emerges.

b. A more accurate calculation

So far we have ignored the contribution to the PV distribution from the relative vorticity of the zonal wind in calculating the temperature distribution. In the following, we obtain the distributions of temperature and wind simultaneously by inverting a given PV distribution under the requirement that mass and momentum are balanced.

1) PV EXPRESSION AND BALANCE EQUATIONS

In the potential temperature–latitude coordinate (θ–ϕ), the PV and the balance equations may be written

$$P_v = -g(f+\zeta_\theta)\left(\frac{\partial p}{\partial\theta}\right)^{-1} \tag{8}$$

$$fU = -\frac{\partial M}{a\partial\phi} \tag{9}$$

$$\Pi(p) = \frac{\partial M}{\partial\theta}, \tag{10}$$

in which $f = 2\Omega\sin\phi$, $\Pi(p) = c_p(p/p_0)^{R_d/c_p}$, $M = c_pT + \Phi$. p is the pressure, $p_0 = 1000$ mb, f is the planetary vorticity, T is the temperature, $\Pi(p)$ is the Exner function, Φ is the geopotential, and M is the Montgomery potential; c_p and R_d are the specific heat and specific gas constants for dry air, respectively. Here U denotes the zonal wind, and

$$\zeta_\theta = -\frac{\partial}{a\partial\cos\phi}U\cos\phi,$$

which is the relative vorticity of the zonal mean flow (Hoskins et al. 1985). Using Eqs. (9) and (10), Eq. (8) can be rewritten as

$$\frac{\partial^2 M}{\partial\phi^2} - \frac{2}{\sin 2\phi}\frac{\partial M}{\partial\phi} + 2\Omega a^2\sin\phi\,\frac{P_v}{g\hat{R}}\frac{\partial^2 M}{\partial\theta^2} + (2\Omega a\sin\phi)^2 = 0 \tag{11}$$

in which

$$\hat{R} = \frac{d\Pi}{dp} = \frac{R_d}{p_0}c_p^{c_v/R_d}\left(\frac{\partial M}{\partial\theta}\right)^{-c_v/R_d}.$$

Thus, Eq. (11) is nonlinear. To emphasize this, we rewrite the equation in the following form:

$$\frac{\partial^2 M}{\partial \phi^2} - \frac{2}{\sin 2\phi}\frac{\partial M}{\partial \phi} + 2\Omega a^2 \sin\phi \frac{P_v}{g}\frac{p_0}{R_d} c_p^{-c_v/R_d} \times \left(\frac{\partial M}{\partial \theta}\right)^{c_v/R_d} \frac{\partial^2 M}{\partial \theta^2} + (2\Omega a \sin\phi)^2 = 0. \quad (12)$$

Equation (12) is a second-order elliptic equation for a positive PV distribution. Note that when the relative vorticity is ignored, Eq. (12) reduces simply to

$$\frac{\partial p}{\partial \theta} = -\frac{gf}{P_v}. \quad (13)$$

Instead, solving Eq. (5) to obtain the temperature distribution as a function of pressure and latitude (as we did in section 3a), one may first obtain the pressure distribution as a function of θ and latitude by solving Eq. (13) and then invert it to obtain the temperature distribution. Note that when PV is homogenized along isentropes, P_v is only a function of θ.

2) AN ILL-POSED PROBLEM

In order to closely examine the calculations presented in section 3a, we choose the surface boundary conditions as a fixed potential temperature distribution and zero wind and leave the upper boundary open. In terms of M, the boundary conditions are

$$M = 0 \quad \text{at} \quad \theta = \theta_s(p_s, \phi)$$

$$\frac{\partial M}{\partial \theta} = \Pi(p_s) \quad \text{at} \quad \theta = \theta_s(p_s, \phi) \quad (14)$$

in which p_s is the surface level pressure. Notice that with a nonzero gradient of potential temperature, the lower surface, defined by a constant pressure, appears in the $(\theta - \phi)$ plane as a curve whose shape is related to the exact distribution of surface temperature. Equation (12) with boundary condition (14) constitutes an ill-posed problem in the following sense. The solution exists and is unique, but is not continuously dependent on the surface temperature distribution (Garabedian 1964). Physically, this is related to the fact that adjustment between the mass and momentum distribution is mutual. Suppose a perturbation is introduced into the potential temperature distribution at the surface level after a state that satisfies Eq. (12) is established; the subsequent adjustment to a new balanced state will involve changes of both temperature and wind. Fixing both of them at a line is physically impossible. As is well known for elliptic-type equations, the boundary generally needs to be closed. Therefore, we must supply an upper boundary condition and lateral boundary conditions at the polar and the tropical extremities. This suggests as well that the role of the stratosphere will have to be taken into account when the wind is also a variable to be solved for.

3) THE EFFECT OF THE ZONAL WIND

To estimate the error introduced by ignoring the relative vorticity of the zonal wind, we need to quantify the differences between the balanced mass and momentum (temperature and wind) distributions corresponding to the two PV distributions presented in Fig. 5. The balanced temperature and wind distributions corresponding to the PV distribution in the lower portion of Fig. 5 are just those in Figs. 3 and 4 (top). What we need is to obtain the balanced temperature and wind distributions corresponding to the PV distribution presented in the upper portion of Fig. 4.

To invert the PV distribution presented in the lower portion of Fig. 5, we need four boundary conditions. To compare with the approximate calculation presented above, we demand that the vertical distribution of wind at 80°N, the vertical distribution of potential temperature at the tropical boundary, and the meridional distributions of potential temperature at the lower and at the upper boundary are the same as those in the approximate calculation.

In mathematical terms, these boundary conditions are

$$\left.\frac{\partial M}{\partial \theta}\right|_{\theta=\theta_s(p_s,\phi)} = \Pi(p_s) \quad (15)$$

$$\left.\frac{\partial M}{\partial \theta}\right|_{\theta=\theta_t(p_t,\phi)} = \Pi(p_t) \quad (16)$$

$$M|_{\phi=\phi_r} = M_r(\theta) \quad (17)$$

$$\left.\frac{\partial M}{a\partial \phi}\right|_{\phi=\phi_l} = -f(\phi_l)U_l(\theta), \quad (18)$$

where p_s and p_t are the pressures that define the vertical domain. Here p_s and p_t represent the lower boundary pressure and the upper boundary pressure, respectively. They can vary with latitude. Further, θ_s and θ_t are the potential temperature distributions at the lower and upper boundary, respectively. They are in general functions of latitude. M_r is the Montgomery potential at the tropical boundary. For a given vertical distribution of temperature and a reference value, it is uniquely determined. U_l is the wind at 80°N.

Equation (12) with the boundary conditions (15), (16), (17), and (18) can be solved based on the traditional nonlinear overrelaxation methods (Ames 1977). Numerical techniques to force the solution to satisfy the lower and the upper boundary conditions are given in detail in appendix B. The numerical method can be directly applied to study the structure of an axially symmetric baroclinic vortex. To expand to three-dimensional flow is also straightforward. The advantage of this inversion for a given PV distribution in potential temperature coordinates is threefold: first, it does not require the coordinate transformation such as

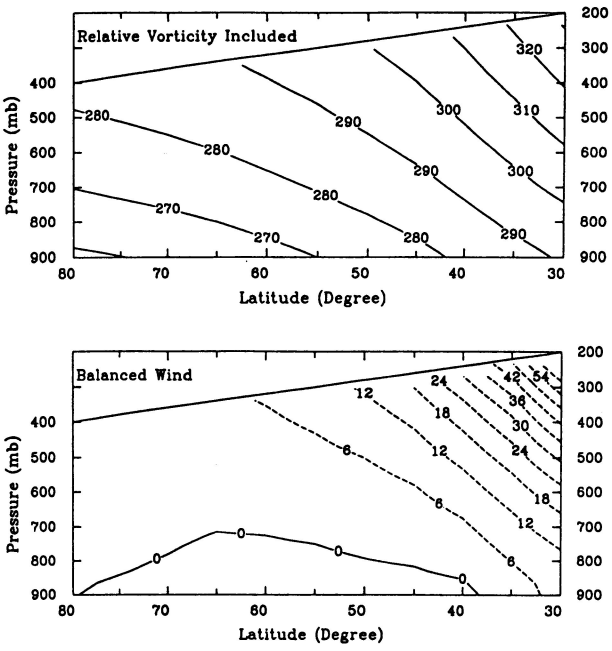

FIG. 6. The distributions of potential temperature and wind obtained by inverting a PV distribution with no gradient along isentropes. Meridional temperature distribution at the surface and at the upper boundary are the same as in Figs. 3 and 4 (top). The tropical lapse rate and the wind at 80°N are also the same as in Figs. 3 and 4 (top).

is needed in semigeostrophic theory; second, it does not involve further approximation in the expression for PV in addition to the balance requirement; finally, it can be used to study the momentum and mass distributions as a function of PV gradient along isentropic surfaces, which directly relates to the instability of the balanced flow (the balanced flow may be either the zonal mean flow or a synoptic-scale vortex).

When the upper boundary is not a surface of constant pressure, the numerical difficulty is greater. For our present purpose, which is to check whether the small differences in the two PV distributions in Fig. 4 will lead to considerable differences in the corresponding balanced temperature and wind distributions, it is not necessary to choose a sloping upper boundary. Note that the approximate calculation does not require knowledge of the position of the tropopause. Instead, assuming that the solution to Eqs. (5) and (6) extends to a region such as shown in Fig. 4, we can assume that the solution extends to the 200-mb level at all latitudes. We then solve Eq. (12) over a region that is slightly higher than the region of interest. For any given potential temperature distribution at the 200-mb level, there will be a corresponding temperature distribution at the sloping tropopause.

By solving Eq. (12) with the boundary conditions, we obtain the distribution of M as a function of latitude and pressure. We then use the balance equations (9) and (10) to obtain the pressure and wind distributions as functions of latitude and potential temperature. Finally, we obtain potential temperature and wind distributions in the pressure and latitude coordinates. The balanced temperature and wind distributions corresponding to the PV distribution in the upper portion of Fig. 5 are presented in Fig. 6. The tropopause pressure is again specified as a linear function of latitude. In the calculation, we chose a higher vertical domain, which is bounded by a constant pressure surface (200 mb). Figure 6 only shows the section below the sloping tropopause, which is what we are interested in. Recall that the present purpose is to estimate the error introduced in obtaining the tropospheric temperature and wind by ignoring the relative vorticity in the PV expression.

We see that both the temperature and wind are quite similar to the approximate solution obtained while ignoring the contribution to the potential vorticity distribution by the zonal wind. In fact there is no distinguishable difference between the temperatures. Weak (no larger than 2 m s^{-1}) easterlies occur at surface level at high latitudes. The surface wind turns out to be very sensitive to the temperature distribution at the tropopause, as we will show shortly.

For a solution with U_l set to zero, no significant change was found to occur.

4) TROPOPAUSE TEMPERATURE AND SURFACE-LEVEL WIND

Figure 7 shows the sensitivity of the wind distribution to changes in the temperature distribution at the tropopause. The cross-isentrope PV distributions for the two cases in Fig. 7 are the same. Their boundary conditions are also the same except that their temperature distribution at the upper boundary is slightly different, which leads to a slightly different distribution at the specified tropopause level (also shown in Fig. 7). This small difference in the temperature distribution leads to a dramatic change in the wind distribution. The solution with easterly winds over the bulk of the extratropics is unrealizable in nature, because there is no way to satisfy the global momentum budget when surface friction is considered. On the one hand, this example demonstrates that the tropopause temperature cannot be accurately determined unless the global momentum balance is considered. On the other hand, since *wind distribution* is so sensitive to a small change in the *temperature structure, the requirement for the global momentum balance* has no practical impact in determining the temperature structure. This suggests that modeling can be simplified if one's concern is only with temperature. The physical reason for the negligible effect of wind distribution on the temperature distribution is that over planetary scales, the relative vorticity is more than one order smaller than the planetary vorticity. This is obviously dependent on the magnitude of the wind, and more fundamentally on the meridional

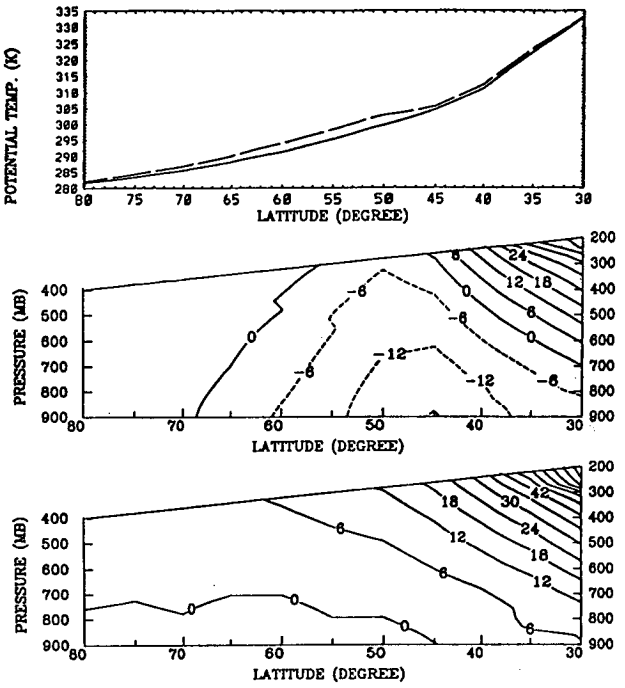

FIG. 7. Sensitivity of the meridional wind distribution to changes in the meridional distribution of the tropopause temperature. Top: Two different meridional distributions of potential temperature at the tropopause. Middle: The balanced wind distribution corresponding to the dashed line in the top figure. Bottom: The balanced wind distribution corresponding to the solid line in the top figure. The zonal winds at 80°N are assumed to be zero for both cases. See text for more details.

temperature gradient. For a much larger pole to equator temperature difference, the wind effect may not be negligible. That the relative vorticity is much smaller than the planetary vorticity is equivalent to $\Delta\theta/\theta_0 \ll (\Omega a/C_0)^2$, where $\Delta\theta$ is the pole to equator temperature difference, θ_0 is the mean tropospheric potential temperature, Ω is the angular velocity of the earth, a is the earth's radius, $C_0 = (gH_0)^{1/2}$, g is the gravitational acceleration, and H_0 is the tropopause height.

Note that once the temperature distribution at the tropopause level is fixed, the role of the stratospheric PV and its gradient in affecting the tropospheric temperature and wind is implicitly taken into account. A fixed tropopause temperature gradient in the meridional direction is equivalent to an infinite meridional gradient of PV (Bretherton 1966). In addition, with the temperature distribution at the tropopause fixed, the perturbation of temperature induced by a PV anomaly in the stratosphere must be zero at the tropopause. Mathematically, the situation can be accounted for by introducing a PV anomaly with the opposite sign in the troposphere. Thus, with the tropopause temperature distribution fixed, any change in stratospheric conditions will be instantaneously reflected in the troposphere.

We note that in the extreme case of complete PV mixing on isentropes, the extratropical zonal mean flow is dependent on the following parameters: the surface temperature distribution, the cross-isentrope PV distribution, position of the tropical boundary, and the tropical lapse rate. In the following sections, we explore rather briefly the sensitivity of the temperature and wind distribution of the zonal mean flow with zero PV gradient to changes in the tropics and in the cross-isentropic PV distribution.

4. Sensitivity to changes in the tropics and in the cross-isentrope PV distribution

We use the same procedures as presented in section 3b to obtain the temperature and balanced wind distributions. For a given surface-level temperature distribution, a given temperature distribution at the tropical boundary, and a given PV distribution across the isentropes originating from the extratropical surface, we first solve Eqs. (5) and (6) to obtain the temperature distribution at the upper boundary (200 mb) and the vertical distribution of wind at 80°N, which will be used as two of the four boundary conditions [Eqs. (15), (16), (17), and (18)] to invert the PV [Eq. (12)] to obtain the balanced temperature and wind distribution. The temperature distribution differs little from the solution of Eq. (5).

a. Sensitivity to the vertical distribution of PV/lapse rate in the tropics

We first examine the sensitivity of the temperature and wind to the vertical distribution of PV at the tropical boundary. When wind shear is small, PV is mainly determined by the lapse rate. Figures 8 and 9 show the temperature and the balanced wind distributions for two cases corresponding to different vertical distributions of PV at the tropical boundary. In one case, the PV at the tropical side boundary is assumed to be well mixed with height, and in the other case it is assumed to increase slightly with height. In both cases, the surface temperature distribution is the same. The PV distribution across the isentropic surfaces originating at the extratropical ground are assumed to increase linearly with latitude from the value at the tropical boundary to the value of 1 PVU at 80°N. We see that a slight change affects both the temperature and wind significantly. The slope of those isentropes that originate from the tropics has a smaller value in the case of constant PV at the tropical boundary. The magnitude and the width of the jet are approximately the same, but there are considerable differences in the detailed spatial distribution of the wind.

b. Sensitivity to the position of the tropical boundary

For simplicity, we assumed that the thermal structure within the domain of the Hadley circulation can be

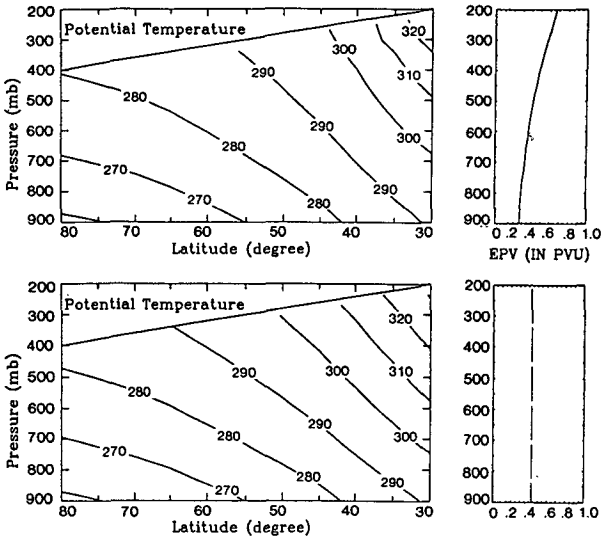

FIG. 8. Sensitivity of the temperature distribution in the extratropical troposphere to the vertical distribution of PV at the tropical boundary. To the right of the potential temperature distributions are the corresponding PV distributions at the tropical boundary.

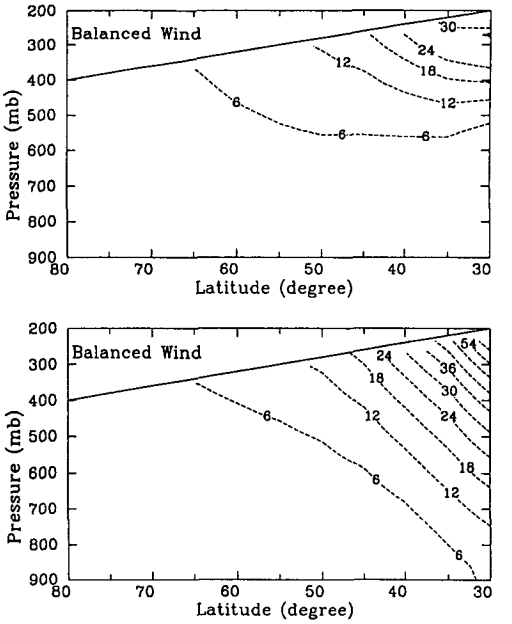

FIG. 9. Sensitivity of the wind distribution in the extratropical troposphere to the vertical distribution of PV at the tropical boundary. The corresponding PV distributions are the same as in Fig. 8.

characterized by a fixed surface temperature and a constant $\partial\theta/\partial p$ (the moist-adiabatic assumption may be more appropriate, but the difference between them is small). The pole to equator temperature difference is assumed to be fixed and the surface temperature distribution outside of the tropics is assumed to be linear with latitude. We also assume that the tropopause height is a linear function of latitude. Furthermore, we assume that the PV distribution across the isentropes originating from the extratropical surface P_{as} increases linearly from the value at the poleward edge of the Hadley circulation to 1.0 PVU at 80°N. These assumptions may artificially restrict the freedom of the extratropical climate to respond to changes in the position of the tropical boundary. These issues, however, cannot be addressed adequately without considering the radiative budget, ocean transport, and the dynamics of the surface boundary layer—all of which are beyond the scope of the present paper. Using these assumptions, the change in the position of the poleward edge of the Hadley circulation affects extratropical temperature and wind by changing the PV value along the isentropic surfaces originating from the tropics, and by changing the meridional distribution of surface temperature and P_{as}. The sensitivity of the extratropical temperature and wind to the position of the tropical side boundary is shown in Figs. 10 and 11. From Figs. 10 and 11, we see that the differences again are primarily limited to the upper troposphere at lower latitudes. For a smaller width of the domain of the Hadley circulation, the PV to be mixed into the middle latitudes along the isentropes originating from the domain of the Hadley circulation is smaller. Consequently, the vertical stability becomes smaller in the region traversed by the isentropes originating from the tropics. In addition, there are also significant differences in the balanced wind distribution.

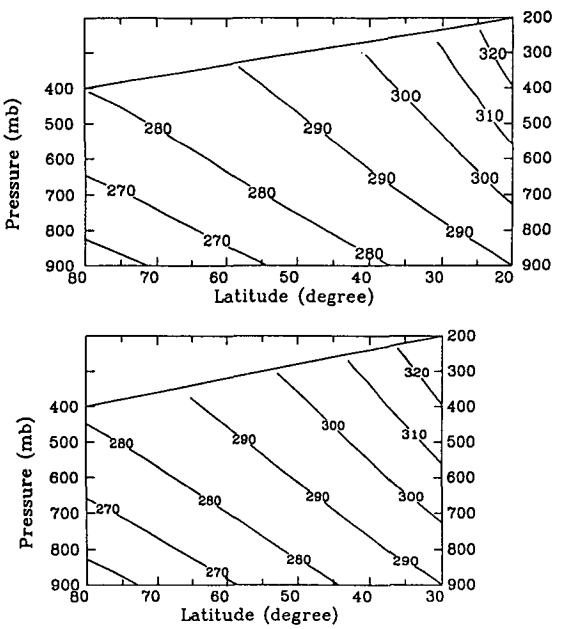

FIG. 10. Sensitivity of temperature distribution in the extratropical troposphere to the position of the tropical boundary. See text for details.

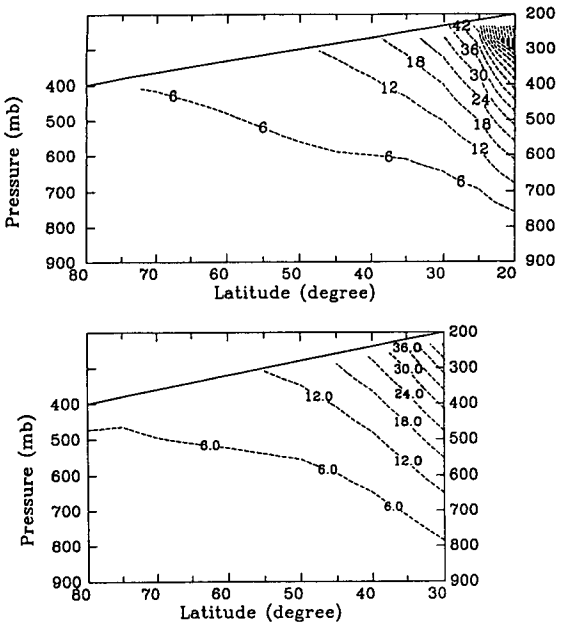

FIG. 11. Sensitivity of the wind distribution in the extratropical troposphere to the position of the tropical boundary. See text for details.

c. *Sensitivity to the PV distribution across the isentropes originating from the extratropical surface*

Figures 12 and 13 show the dependence of temperature and wind on P_{as}, the PV distribution across the isentropes originating from the extratropical surface. The PV value on each isentropic surface originating from the tropics is assumed to be uniform and the same in the two cases. The meridional distributions of potential temperature at 900 mb for the two cases are also the same. Though the larger the PV, the larger the vertical stability, it is interesting to note that the effect on the vertical stability is not local because of the efficient transport of PV along isentropic surfaces. The jet structures in the two figures are almost the same, which shows that the jet is mainly determined by the PV distribution on the isentropes originating from the tropics. Figures 12 and 13 also show that the meridional distribution of P_{as} slightly affects the slopes of those isentropes originating from the tropics. It appears that the larger the meridional gradient of P_{as}, the higher the latitude to which an isentrope originating from the tropics can penetrate before it reaches the tropopause, though the dependence of the slope of the isentropes originating from the tropics on the meridional distribution of P_{as} is not strong.

In the above investigations, we have focused on the case with zero PV gradient. Since a flow with zero PV gradient and a proper elevation of the tropopause is neutral for baroclinic eddies, it is also the limit that the flow may tend to. In the following section, we examine the sensitivity of the temperature and wind distribution of the zonal flow to changes in the PV gradient along isentropes. The diabatic effects associated with latent heat release, radiation, and the intrusion of stratospheric air will tend to generate PV gradients along isentropic surfaces. Precise neutrality is not expected. To quantify the dependence of the tropospheric temperature and wind distributions on the PV gradient along isentropic surfaces is potentially an effective way to estimate the stratospheric influence and the diabatic effects.

5. Sensitivity to PV gradients along isentropic surfaces

To simplify Eq. (3), we shall assume the gradient of PV can be written in the following form,

$$\left(\frac{\partial P}{\partial y}\right)_{\theta} = -g\alpha(y)\frac{\partial \theta}{\partial p} \tag{19}$$

where $\alpha(y)$ corresponds to the QGPV gradient. When $\partial\theta/\partial p$ can be replaced by a reference value, α is exactly the gradient of QGPV (Charney and Stern 1962).

With this constraint, Eq. (3) can be simplified to

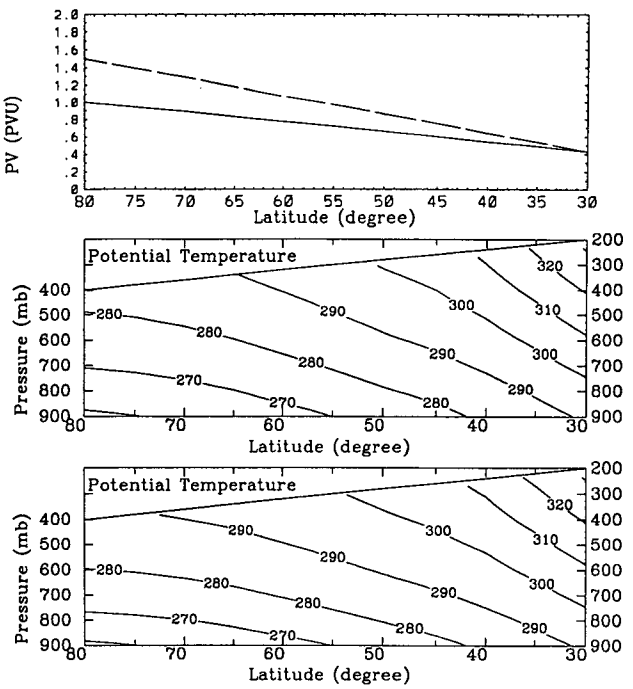

FIG. 12. Sensitivity of temperature distribution in the extratropical troposphere to the meridional distribution of PV across the isentropes originating from the extratropical surface (P_{as}). Top: The two different meridional distributions of P_{as}. Middle and bottom: The corresponding distributions of potential temperature. The middle figure corresponds to the solid line in the top figure, and the bottom figure corresponds to the dashed line in the top figure. See text for details.

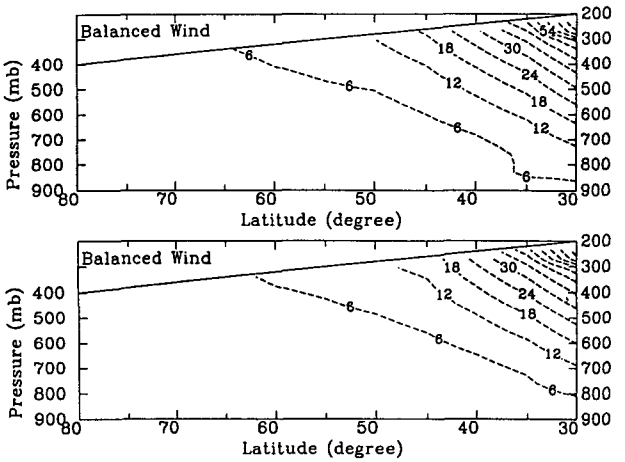

FIG. 13. Sensitivity of wind distribution in the extratropical troposphere to the meridional distribution of PV across the isentropes originating from the extratropical surface (P_{as}). The top figure corresponds to the solid line in the top panel of Fig. 12, and the bottom figure corresponds to the dashed line in Fig. 12. See text for details.

$$f\frac{\partial\theta}{\partial y} - \left(\frac{-gf^2}{P_{as}}\frac{\partial\theta_s}{\partial y} + (\alpha - \beta)(p - p_s)\right)\frac{\partial\theta}{\partial p} = 0 \tag{20}$$

in which $\beta(y) = df/dy$, the planetary vorticity gradient.

We employ the same procedure as in section 4. For a given surface-level temperature distribution, a given temperature distribution at the tropical boundary, and a given cross-isentrope PV distribution at the surface level, we first solve Eqs. (20) and (6) to obtain the temperature at the upper boundary and the wind at 80°N. Using this temperature and wind as the upper boundary condition and the polar boundary condition, respectively, for solving Eq. (12), we obtain the balanced mass and momentum distributions. Potential temperature and the balanced wind distributions corresponding to $\alpha(y) = \beta(y)$ and $\alpha(y) = 2\beta(y)$ are presented in Figs. 14 and 15. Their PV distributions are shown in Fig. 16. The surface level temperature and PV distribution for Figs. 15 and 16 are the same as for the top panel of Fig. 3. Compared with the case with zero gradient, the isentropic slope is smaller and the tropopause temperature is warmer. The maximum wind is also smaller. So far as the slope of those isentropic surfaces originating from the tropics is concerned, the presence of the PV gradient actually helps more heat to be transported to high latitudes. Note that this is not to say the presence of the planetary vorticity gradient makes the equator to pole heat transport more efficient. As we have already seen in section 3, it is precisely the increase of planetary vorticity that causes the slope of the isentropic surfaces to increase with height when there is no PV gradient along isentropic surfaces.

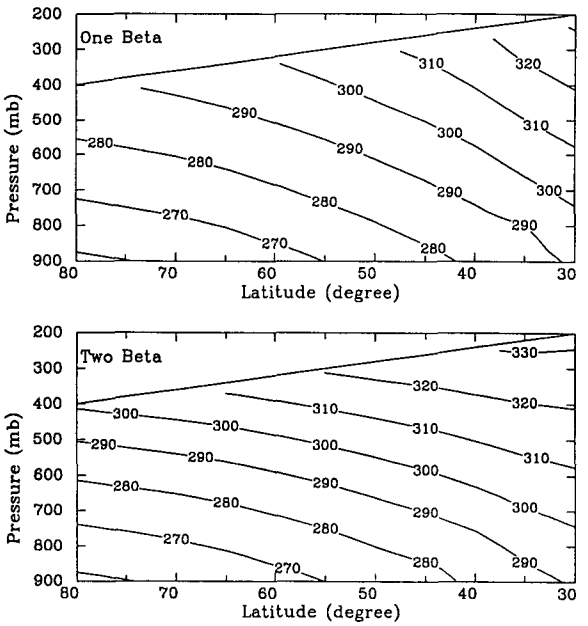

FIG. 14. Potential temperature distribution corresponding to $\alpha = \beta$ and $\alpha = 2\beta$. The surface temperature distribution and the tropical lapse rate are the same for the two cases.

The major difference from the case with zero gradient occurs at the jet region, which suggests the importance of the presence of a positive gradient of PV there for a warmer upper troposphere.

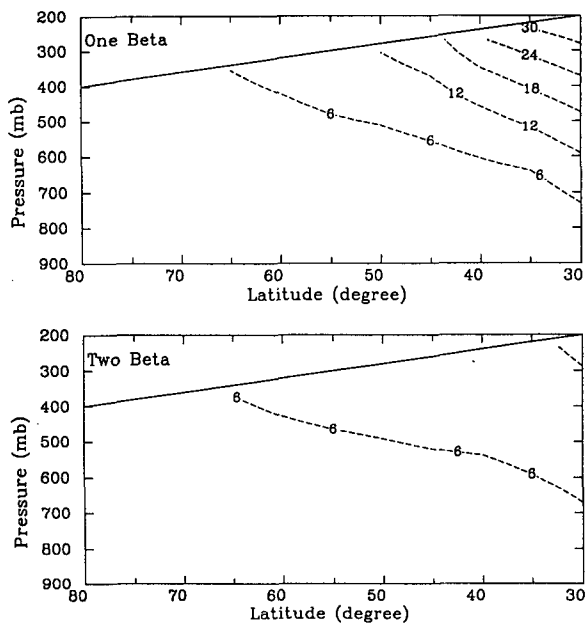

FIG. 15. Wind distribution corresponding to $\alpha = \beta$ and $\alpha = 2\beta$. The surface temperature distribution and the tropical lapse rate are the same for the two cases.

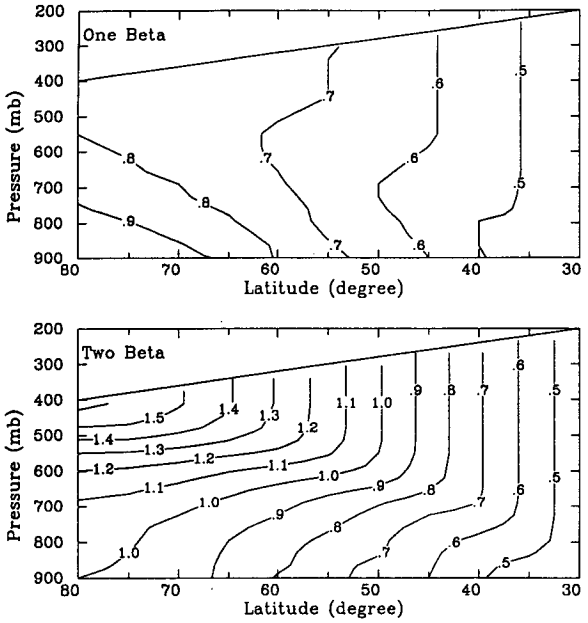

FIG. 16. PV distributions corresponding to the temperature and wind distributions in Figs. 14 and 15.

6. Summary

We have studied the dependence of the distribution of temperature and wind of the zonal mean flow in the extratropical troposphere on the gradient of PV along isentropes. In particular, we have examined the difference between the temperature and wind distribution of a troposphere with a constant PV along isentropes and the observed. We have also investigated the implications of PV homogenization along isentropes for the role of the tropics.

The distributions of PV along isentropes of the observed zonal mean flow indicate mixing in the interior of the extratropical troposphere. For the same surface temperature distribution, extratropical zonal mean flow with zero PV gradients along isentropes is close to the observed except in the upper troposphere adjacent to the Hadley circulation. These results suggest that the PV in the extratropical troposphere indeed tend to be homogenized. The question that remains to be explored further is why this homogenization occurs. Lindzen's note (1993) provides a plausible mechanism. There is hardly any question that eddies resulting from instability will *tend* to neutralize the flow. Given that the surface-level temperature is related to SST and its meridional gradient is hard to completely eliminate by baroclinic eddies, neutralization by eliminating internal PV gradients while elevating the tropopause as defined by the level where PV gradients are concentrated (Lindzen 1993) is an appealing mechanism. As to how close the time-mean structure should be to a completely neutralized state is a separate issue and cannot be addressed appropriately without considering the nature of the forcing and dissipation.

The results of this paper also suggest that one may effectively parameterize the collective effect of baroclinic eddies by assuming that they homogenize PV along isentropes. This parameterization may offer a better means than models based on the QG theory to examine the maintenance of the vertical stability of the extratropical troposphere and the interaction between the Hadley circulation and the baroclinic eddies. Due to the assumptions built into the QG theory, QG models cannot appropriately address the maintenance of the vertical stability and the role of the tropics. The lapse rate feedback and pole to equator temperature difference are among the leading factors that determine the climate sensitivity to radiative perturbations.

Some quantitative difference between the extratropical troposphere with zero PV gradient and the observed exists, particularly in the upper troposphere adjacent to the Hadley circulation. Compared with the observed, the extratropical troposphere with zero PV gradient has a larger isentrope slope and a stronger meridional temperature gradient in the upper troposphere. The upper troposphere is considerably colder and the latitude that the isentropes originating from the tropics can penetrate to before they reach the tropopause is also smaller. It appears that an efficient PV mixing along isentropes may not help the tropics to have more impact on the extratropics.

Resulting from a larger isentrope slope and a stronger meridional temperature gradient, the thermal wind is also stronger. Assuming the surface-level wind remains close to zero or westerly, the neutralized troposphere will have a stronger jet than the observed. This may have some new implications for the maintenance of the subtropical jet. In the absence of eddies and in the inviscid limit, the Hadley circulation produces a stronger jet than the observed (Held and Hou 1981). It has been suggested that the inclusion of baroclinic eddies will contribute to weakening the jet (Pfeffer 1981; Hoskins 1983). Indeed, this may be possible if the intense eddies restrict the extent of the Hadley circulation. However, stronger baroclinic eddies will also tend to cause PV to be better mixed along isentropes. In both cases, other factors such as the vertical mixing by cumulus convection and the intensity of the Hadley circulation will play an important role.

The differences between the case with PV well mixed along isentropes and the observed presumably result from the nonnegligible effects of the local diabatic and frictional processes in the real atmosphere. It will be of interest in future studies to quantify the relationship between the PV gradient along isentropes of an equilibrium state and the diabatic and frictional parameters.

Near the tropical boundary, the Hadley circulation plays a major role in maintaining a PV gradient. In the absence of the eddies, the Hadley circulation creates a

very large PV gradient at its edge (Held and Hou 1981; Lindzen and Hou 1991) through homogenization of PV within the domain of the Hadley circulation. The knowledge of the balance between creating and destroying the PV gradient at the edge of the Hadley circulation may be essential for determining where the Hadley circulation ends in the presence of eddies.

Given the clear constraint of the global angular momentum balance on the meridional distribution of the zonal wind (surface wind in particular), one may expect that this constraint may also affect the temperature in a significant way. Indeed, our results suggest that even in the extreme case of complete PV mixing, the meridional temperature distribution at the tropopause cannot be determined without referring to the global momentum balance. However, we found that the surface wind distribution is very sensitive to changes in the tropopause temperature distribution. Relatedly, the requirement of global momentum balance has negligible effects on the temperature distribution. This offers support for the use of energy balance models when the temperature structure is the major concern. Nevertheless, the exact distribution of the meridional wind may play an important role in determining the tropopause height in the manner noted by Lindzen (1993); namely, the width of the jet limits the horizontal scale of the unstable baroclinic eddies.

Assuming the PV gradient remains zero, we further found that the temperature and wind distribution of the extratropical troposphere is sensitive to the vertical distribution of PV (or lapse rate) at the edge of the Hadley circulation. With a surface temperature distribution which is linear with latitude, we found that the jet maximum occurs at the tropical boundary and moves with it. The overall pattern of the temperature and wind distribution does not seem to be very sensitive to the change of the position of the tropical boundary.

Another interesting finding of this study is that the larger the PV gradient along isentropes, the warmer the tropopause. This implies that an efficient homogenization of PV along isentropes is not equivalent to efficient heat transport at all levels.

Finally it should be noted that the lapse rate (or PV along isentropes) in the extratropical troposphere is a function of both the surface temperature distribution and the temperature of the tropics. This dependence can be determined by applying the radiative constraint (i.e., the requirement for the global energy balance). Considering the dynamic significance of the zonal mean flow with no PV gradient along isentropes and its closeness to the present observed world, it would be a useful exercise to investigate the sensitivity of this zonal mean flow to radiative perturbations. This is an issue that we will explore in the future.

Acknowledgments. This paper was a part of the thesis research of the first author (D.-Z. Sun). It was supported by the National Science Foundation under Grant ATM-914441, and by the National Aeronautics and Space Administration under Grant NAGW-525. Part of the final writing was done while D.-Z. Sun was a visiting scientist of the Program in Atmospheric and Oceanic Sciences at Princeton University. We gratefully acknowledge the helpful discussions with Professors A. Plumb, K. Emanuel, P. Stone, and R. Prinn at MIT and Dr. I. Held at GFDL. We also wish to thank P. Tunison at GFDL, who helped draft some of the figures.

APPENDIX A

A Numerical Scheme for Solving Equation (5)

Equation (5) has the form

$$\frac{\partial \theta}{\partial y} - s(y,p)\frac{\partial \theta}{\partial p} = 0. \tag{A1}$$

Using a one-step backward difference to discretize the derivative of θ in both y and p direction, we have the difference form of Eq. (A1),

$$\theta(i,j) = \theta(i-1,j) + C(i,j)(\theta(i-1,j) - \theta(i-1,j-1)), \tag{A2}$$

with $C(i,j) = S(i,j)\delta y/\delta p$. It is easy to show that the stability criterion for the above scheme is

$$|C(i,j)|_{\max} < 1. \tag{A3}$$

APPENDIX B

A Numerical Scheme for Solving Equation (12)

Equation (12) has the form

$$A(y,z)\frac{\partial^2 U}{\partial y^2} + E(y,z)\frac{\partial U}{\partial y} + S(y,z)\left(\frac{\partial u}{\partial z}\right)^{\gamma}\frac{\partial^2 U}{\partial z^2} + Q(y,z)\frac{\partial U}{\partial z} + C(y,z) = 0. \tag{B1}$$

The boundary conditions it is subject to are

$$\left.\frac{\partial U}{\partial z}\right|_{z=z_1(y)} = T_1(y) \tag{B2}$$

$$\left.\frac{\partial U}{\partial z}\right|_{z=z_2(y)} = T_2(y) \tag{B3}$$

$$U|_{y=y_1} = U_1(z) \tag{B4}$$

$$\left.\frac{\partial U}{\partial y}\right|_{y=y_2} = U_{y_0}, \tag{B5}$$

where $z = z_1(y)$, $z = z_2(y)$, $y = y_1$, and $y = y_2$ define a closed domain. The domain and the discrete grid that we use to discretize the domain for Eq. (B1) and its boundary conditions are schematically shown in Fig. B1.

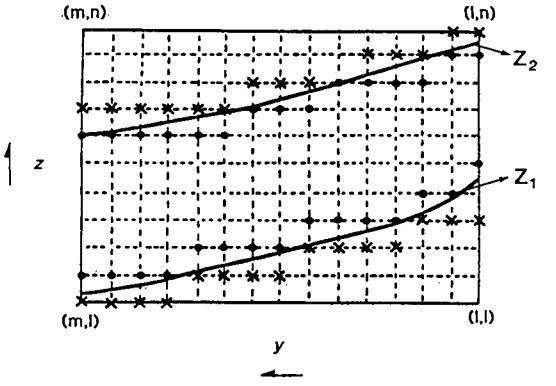

FIG. B1. The grid used to discretize the elliptic equation and its boundary conditions. The dots denote the inner boundary points.

In general $z = z_1(y)$ and $z = z_2(y)$ are not orthogonal to the two parallel lines $y = y_1$ and $y = y_2$, and may not be straight lines in the y–z plane. In the rectangular grid, $z = z_1(y)$ and $z = z_2(y)$ may be represented by the mesh points closest to them, including the points that fall right on the boundary curves. These points are called boundary points and may be further divided into the inner boundary points and outer boundary points. The inner boundary points are those points that fall either inside the domain or right on the boundary curve. The outer boundary points are those that fall just outside the domain. Other points within the closed domain will be called interior points. We use arrays $J_1(i)$ and $J_2(i)$ $(i = 1, m)$ to denote the inner boundary points that are associated with the boundary curves $z = z_1(y)$ and $z = z_2(y)$, respectively. They are represented by dots shown in Fig. 13. Here we restrict ourselves to the case in which both $z_1(y)$ and $z_2(y)$ decrease monotonically with y.

The equation can be solved by overrelaxation methods. Let "k" denote the iteration step, α represent the overrelaxation parameter, and let the iteration proceed from $[1, J_1(1)]$, column by column to the point $[m, J_2(m)]$.

At the interior points [they are denoted by (i, j)], we have

$$V^k(i,j) = \left[2\left(A(i,j) + B(i,j)\left(\frac{\delta y}{\delta z}\right)^2\right)\right]^{-1}\left[A(i,j)(U^{k-1}(i+1,j) + U^k(i-1,j)) + \frac{1}{2}E(i,j)(U^{k-1}(i+1,j) - U^k(i-1,j))\delta y + B(i,j)(U^{k-1}(i,j+1) + u^k(i,j-1))\left(\frac{\delta y}{\delta z}\right)^2 + \frac{1}{2}Q(i,j)(U^{k-1}(i,j+1) - U^k(i,j-1))\delta z^{-1}(\delta y)^2 + C(i,j)\delta y^2\right]$$

$$U(i,j)^k = U(i,j)^{k-1} + \alpha V^k(i,j); \tag{B6}$$

$B(i,j) = S(i,j)R(i,j)$ and $R(i,j)$ are given by

$$R(i,j) = \left[\frac{(U^{k-1}(i,j+1) - U^k(i,j-1))}{2\delta z}\right]^\gamma \quad \text{for} \quad j < J_2(i-1)$$

$$R(i,j) = \left[\frac{(U(i,j)^{k-1} + T(i)\delta z - U^k(i,j-1))}{2\delta z}\right]^\gamma \quad \text{for} \quad j = J_2(i). \tag{B7}$$

At the boundary points, we have the following situations:

At $y = y_2$, and for $J_1(m) < j < J_2(m)$:

$$V^k(m,j) = \left[2\left(A(m,j) + B(m,j)\left(\frac{\delta y}{\delta z}\right)^2\right)\right]^{-1}\left[A(m,j)(2U^k(m-1,j) + 2U_{y_0}(j)\delta y) + E(m,j)U_{y_0}(j)\delta y^2 + B(m,j)(U^k(m,j-1) + U^{k-1}(m,j+1))\left(\frac{\delta y}{\delta z}\right)^2 + \frac{1}{2}Q(m,j)(U^{k-1}(m,j+1) - U^k(m,j-1))\delta y\delta y\delta z^{-1} + C(m,j)\delta y\delta y\right]$$

$$U(m,j)^k = U(m,j)^{k-1} + \alpha V^k(m,j). \tag{B8}$$

For $j = J_1(m)$:

$$V^k(m,j) = \left[2A(m,j) + B(m,j)\left(\frac{\delta y}{\delta z}\right)^2\right]^{-1}\Big[A(m,j)(2U^k(m-1,j) + 2U_{y_0}(j)\delta y) + E(m,j)U_{y_0}(j)\delta y^2$$
$$+ B(m,j)(U^{k-1}(m,j+1) - T_1(i)\delta z)\left(\frac{\delta y}{\delta z}\right)^2 + Q(m,j)T_1(i)\partial y^2 + C(m,j)\delta y^2\Big]$$
$$U(m,j)^k = U(m,j)^{k-1} + \alpha V^k(m,j). \tag{B9}$$

For $j = J_2(m)$:

$$V^k(m,j) = \left[2A(m,j) + B(m,j)\left(\frac{\delta y}{\delta z}\right)^2\right]^{-1}\Big[A(m,j)(2U^k(m-1,j) + 2U_{y_0}(j)\delta y) + E(m,j)U_{y_0}(j)\delta y^2$$
$$+ B(m,j)(U^k(m,j-1) + T_2(i)\delta z)\left(\frac{\delta y}{\delta z}\right)^2 + Q(m,j)T_2(i)\delta y^2 + C(m,j)\delta y^2\Big]$$
$$U(m,j)^k = U(m,j)^{k-1} + \alpha V^k(m,j). \tag{B10}$$

For $j = J_2(i)$ and $(J_2(i) > J_2(i+1))$:

$$V^k(i,j) = \left[2A(i,j) + B(i,j)\left(\frac{\delta y}{\delta z}\right)^2\right]^{-1}\Big[A(i,j)(U^{k-1}(i+1, J_2(i+1))$$
$$+ T_2(i+1)(J_2(i) - J_2(i+1))\delta z + U^k(i-1,j)) + \tfrac{1}{2}E(i,j)(U^{k-1}(i+1, J_2(i+1))$$
$$+ T_2(i+1)(J_2(i) - J_2(i+1))\delta z - U^k(i-1,j))\delta y + B(i,j)(U^k(i,j-1)$$
$$+ T_2(i)\delta z)\left(\frac{\delta y}{\delta z}\right)^2 + Q(i,j)*T_2(i)(\delta y)^2 + C(i,j)(\delta y)^2\Big]$$
$$U(i,j)^k = U(i,j)^{k-1} + \alpha V^k(i,j). \tag{B11}$$

For $j = J_2(i)$ and $J_2(i) < J_2(i+1)$ or $J_2(i) = J_2(i+1)$:

$$V^k(i,j) = \left[2A(i,j) + B(i,j)\left(\frac{\delta y}{\delta z}\right)^2\right]^{-1}\Big[A(i,j)(U^{k-1}(i+1,j) + U^k(i-1,j))$$
$$+ \tfrac{1}{2}E(i,j)(U^{k-1}(i+1,j) - U^k(i-1,j))\delta y + B(i,j)(U^k(i,j-1) + T_2(i)\delta z)\left(\frac{\delta y}{\delta z}\right)^2$$
$$+ Q(i,j)*T_2(i)(\delta y)^2 + C(i,j)(\delta y)^2\Big]$$
$$U(i,j)^k = U(i,j)^{k-1} + \alpha V^k(i,j). \tag{B12}$$

For $j = J_1(i)$ and $(J_1(i) < J_1(i-1))$:

$$V^k(i,j) = \left[2A(i,j) + B(i,j)\left(\frac{\delta y}{\delta z}\right)^2\right]^{-1}\Big[A(i,j)(U^{k-1}(i+1,j) - T_1(i-1)(J_1(i-1) - J_1(i))\delta z$$
$$+ U^k(i-1, J_1(i-1))) + \tfrac{1}{2}E(i,j)(U(i+1,j) - (U^k(i-1, J_1(i-1))$$
$$- T_1(i-1)(J_1(i-1) - J_1(i))\delta z)\delta y + B(i,j)(U^k(i,j+1) - T_1(i)\delta z)\left(\frac{\delta y}{\delta z}\right)^2$$
$$+ Q(i,j)*T_1(i)(\delta y)^2 + C(i,j)(\delta y)^2\Big]$$

$$U(i,j)^k = U(i,j)^{k-1} + \alpha V^k(i,j). \tag{B13}$$

For $j = J_1(i)$ and $J_1(i) > J_1(i-1)$ or $J_1(i) = J_1(i-1)$:

$$V^k(i,j) = \left[2A(i,j) + B(i,j)\left(\frac{\delta y}{\delta z}\right)^2\right]^{-1}\left(A(i,j)(U^{k-1}(i+1,j) + U^k(i-1,j))\right.$$
$$+ \frac{1}{2}E(i,j)*(U^{k-1}(i+1,j) - U^{k-1}(i-1,j))\delta y + B(i,j)(U^k(i,j+1) - T_1(i)\delta z)\left(\frac{\delta y}{\delta z}\right)^2$$
$$\left. + Q(i,j)*T_1(i)\delta y^2 + C(i,j)\delta y^2\right]$$

$$U(i,j)^k = U(i,j)^{k-1} + \alpha V^k(i,j). \tag{B14}$$

REFERENCES

Ames, W. F., 1977: *Numerical Methods for Partial Differential Equations.* Academic Press, 365 pp.

Charney, J. G., and M. E. Stern, 1962: On the stability of internal baroclinic jets in a rotating atmosphere. *J. Atmos. Sci.,* **19,** 159–172.

Garabedian, P. R., 1964: *Partial Differential Equations.* Wiley & Sons, 672 pp.

Held, I. M., and A. Y. Hou, 1981: Nonlinear axially symmetric circulations in a nearly inviscid atmosphere. *J. Atmos. Sci.,* **37,** 515–533.

Hoskins, B. J., 1983: Modeling of the transient eddies and their feedback on the mean flow. *Large-Scale Dynamic Processes in the Atmosphere,* B. J. Hoskins and R. Pearce, Eds., Academic Press, 399 pp.

——, 1991: Towards a PV-θ view of the general circulation. *Tellus,* **43A-B,** 27–35.

——, M. E. McIntyre, and A. W. Robertson, 1985: On the use and significance of isentropic potential vorticity maps. *Quart. J. Roy. Meteor. Soc.,* **111,** 877–946.

Hou, A. Y., and R. S. Lindzen, 1992: The influence of concentrated heating on the Hadley circulation. *J. Atmos. Sci.,* **49,** 1233–1241.

Lindzen, R. S., 1993: Baroclinic neutrality and the tropopause. *J. Atmos. Sci.,* **50,** 1148–1151.

Luyten, J. R., J. Pedlosky, and H. Stommel, 1983: The ventilated thermocline. *J. Phys. Oceanogr.,* **13,** 292–309.

Marshall, J. C., and A. J. G. Nurser, 1991: A continuously stratified thermocline model incorporating a mixed layer of variable thickness and density. *J. Phys. Oceanogr.,* **21,** 1780–1792.

Oort, A. H., 1983: *Global Atmospheric Circulation Statistics, 1958–1973.* NOAA Prof. Paper No. 14. NOAA, U.S. Dept. of Commerce, Rockville, MD, 180 pp.

Pedlosky, J., 1987: *Geophysical Fluid Dynamics.* Springer-Verlag, 710 pp.

Pfeffer, R. L., 1981: Wave–mean flow interactions in the atmosphere. *J. Atmos. Sci.,* **38,** 1341–1359.